electronics

Article

Optimal Power Allocation and Cooperative Relaying under Fuzzy Inference System (FIS) Based Downlink PD-NOMA

Asif Mahmood [1,*], Mohamed Marey [1], Moustafa M. Nasralla [1] and Maged A. Esmail [1] and Muhammad Zeeshan [2]

[1] Smart Systems Engineering Laboratory (SSEL), Department of Communications and Networks Engineering, College of Engineering, Prince Sultan University, Riyadh 11586, Saudi Arabia; mfmmarey@psu.edu.sa (M.M.); mnasralla@psu.edu.sa (M.M.N.); mesmail@psu.edu.sa (M.A.E.)

[2] Walton Institute of Information and Communication Systems Science, Waterford Institute of Technology, X91 P20H Waterford, Ireland; muhammad.zeeshan@wit.ie

* Correspondence: amahmood@psu.edu.sa

Abstract: Optimal power allocation (PA) is a decisive part of the power domain non-orthogonal multiple access (PD-NOMA) technique. In PD-NOMA, users are served at the same time and using the same frequency band, but at differing power levels. In this paper, the optimization problem for PA is formulated with distance (d), signal-to-noise ratio (SNR), and foliage depth (d_f) constraints. A fuzzy inference system (FIS) addresses the optimization problem by allocating the optimal power factors (power levels) to each user in the vicinity of a 5G base-station (gNodeB). The proposed system incorporates a cooperative relaying technique at the near-user to assist the far-user facing signal degradation and greater path losses. A realistic 5G micro-cell is analyzed for downlink PD-NOMA where superposition coding (SC) is used at the transmitter side, a successive interference cancellation (SIC) scheme at the near-user, and a maximum ratio combining (MRC) technique at the far-user's receiver, respectively. For both simple PD-NOMA and cooperative relaying PD-NOMA, the presented technique's bit-error-rate (BER) performance is evaluated against various SNR values, and it is concluded that cooperative PD-NOMA outperforms simple PD-NOMA. By combining the presented FIS system with cooperation relaying, the proposed FIS method guarantees user fairness in PD-NOMA systems while also significantly improving performance.

Keywords: PD-NOMA; SIC; cooperative relaying; fuzzy inference system

Citation: Mahmood, A.; Marey, M.; Nasralla, M.M.; Esmail, M.A.; Zeeshan, M. Optimal Power Allocation and Cooperative Relaying under Fuzzy Inference System (FIS) Based Downlink PD-NOMA. *Electronics* **2022**, *11*, 1338. https://doi.org/10.3390/electronics11091338

Academic Editor: Raed A. Abd-Alhameed

Received: 24 March 2022
Accepted: 17 April 2022
Published: 22 April 2022

1. Introduction

The demand for novel wireless communication techniques is at an all-time high to meet capacity targets and envision a new era for 5G and beyond technologies. In this regard, some promising fifth generation (5G) techniques have been acknowledged, such as non-orthogonal multiple access (NOMA) [1–3], interleave division multiple access (IDMA) [4,5], sparse code multiple access (SCMA) [6], low-density spreading multiple access (LDSMA) [7], pattern division multiple access (PDMA) [8], massive multiple input and multiple output (massive MIMO) [9], cooperative communication [10], and so on. Each of the above 5G techniques is unique in its own right and is classified based on a diverse range of quality of service, user fairness, spectral efficiency, low latency, and a diverse degree of freedom.

The power domain NOMA (PD-NOMA) is a 5G wireless technique that incorporates all of the above properties into a single package. In PD-NOMA [11], users around the 5G base-station (gNodeB) are served at the same frequency and time but with varying powers. Considering the downlink PD-NOMA, the superposition coding (SC) is performed at the gNodeB and SIC schemes on the serving user's side. After decoding an undesirable user's signal, the SIC technique [12,13] is used to eliminate its effect by subtracting it from the received signal. The PD-NOMA system has been broadly investigated for a maximum

of two users in [14,15]. To achieve the capacity goals in congested NOMA networks, some recent work has been proposed in [16,17] that effectively addresses the multi-user PD-NOMA systems. The overall performance of PD-NOMA is thoroughly dependent on power allocation (PA) and user clustering techniques. The PA is established through a distance-based power allocation algorithm (DBPA) in [16,18], whereby the near-user is allocated a lower power and the far-user a higher power. User clustering techniques (Best with Best and Best with Poor models) were proposed by Hussain et al. in [19,20]. In the Best with Best model, users having the same channel conditions are grouped into the same cluster, while the Best with Poor model has users in descending order of their channel gains. Orthogonal and non-orthogonal spreading codes such as(Pseudo-Noise (PN) and Walsh codes are used to distinguish equidistant users from the gNodeB in multi-cluster PD-NOMA [18]. As a result, the inter-cluster interference is overcome with the help of spreading codes and intra-cluster interference over the SIC technique.

Consider the practical 5G micro-cells with foliage or vegetation close to the gNodeB, which operates using millimeter wave (mmWave) communication at gigahertz (GHz) frequencies. At such higher frequencies, the mmWave signals are obstructed by small particles. As a result, the signal is attenuated more, which leads to substantial path losses. For the sake of simplicity, we include the foliage part in our simulation because it weakens the signal but does not totally block it, as do buildings wall and other barriers. To address such path loss issues, multiple advanced techniques have been introduced, such as unmanned-aerial-vehicle (UAV) assisted communication [21], re-configurable intelligent surfaces (RIS) or meta-surfaces [22,23] and cooperative communication [24]. UAVs mostly help in providing a direct line-of-sight (DLOS) path between transmitter and receiver where chances of signal blockage and attenuation are reduced effectively. The RIS is installed on the surfaces of building walls to direct the phase-shifted and amplified version of the incident signal with negligible attenuation [25]. To shift the trend in mmWave communication from using probabilistic radio channels to deterministic channel modeling, an efficient radio technique called Ray-tracing [26] is being used nowadays. Ray tracing was first introduced in the 1990s [27] but is currently attracting the attention of most researchers due to its reliability in high-frequency communication. Ray tracing consumes more time at lower frequencies while effectively working at higher frequencies such as in GHz and THz communication [28]. Cooperative relaying is used to enhance the performance of far-users by using the near-users as relay nodes in the system [29].

Moreover, the power optimization problem is a crucial part of PD-NOMA to deal with. In the previously mentioned work, the power allocation has no such dedicated and optimal power allocation strategies. Most of them performed the power allocation process using classical methods such as DBPA, and some used random power factors for PD-NOMA users. The limitation of the previous methods for power allocation strategies such as in [16–18] is the user-fairness. Considering only the distance parameter is not enough for accurate power distribution among NOMA users. However, it is urgently needed to propose a power allocation strategy that is optimal and ensures user-fairness. To address this issue, we are proposing a human intuition-based fuzzy inference system approach that not only considers the distance separation of users from the gNodeB but also incorporates other parameters as well, such as signal-to-noise ratio (SNR) and foliage depth (d_f) during the power allocation process. The purpose of considering these multi-input parameters is to make the power allocation process accurate and optimal so that each user is served with equity and fair-play during power distribution. For the allocation of relay nodes, a fuzzy logic-based method is utilized, which effectively improves the choice of adaptive data rates and assigning power for NOMA transmission in [30]. To optimize the productivity of conventional and complex fuzzy systems, the Mamdani complex fuzzy inference system (Mamdani CFIS) was developed by Selvachandran et al. in [31]. It has been shown that the suggested Mamdani CFIS is simpler, faster, and provides a more efficient way of dealing with time information and time-periodic events than any other fuzzy IS identified in the literature to date. Similarly, the Fuzzy-System Kernel Machines,

a family of machine learning techniques concerning the relationship of FIS systems and kernel machines, were introduced by Guevara et al in [32]. The fundamental motivation for utilizing FL to solve these problems is that they are difficult to model with mathematical equations. Instead, systems that replicate people's behaviors can easily manage them. Power control, traffic control, and channel selection are some of FL's application fields. Cellular systems and bandwidth allocation in cognitive radio networks [33,34] are two notable areas where FL is productive. An approach to generating a fuzzy inverse matrix has been introduced in [35]. Using this method, the fuzzy system is turned into an identical structure of crisp polynomial equations. The eigenvalue approach is used to calculate the solutions to the crisp polynomial equations. Fuzzy systems have a wide range of applications [36–40]. In [40], a fuzzy inference system is used in the medical field for the intensive care of patients where depth of anesthesia (DOA) estimation approach is designed using a machine learning algorithm and an adaptive neuro-fuzzy model.

This paper presents two different and important aspects of PD-NOMA in 5G-based micro-cells: optimal PA and cooperative relaying. We developed a fuzzy logic-based system that assigns each PD-NOMA user the optimal power levels. Furthermore, we incorporate a cooperative relaying technique into the PD-NOMA system that effectively addresses the raised issues at far-user due to intense path losses. The proposed paper's primary contributions are as follows;

- The power optimization problem is coordinated through multi-input parameters such as distance (d), signal-to-noise ratio (SNR), and foliage depth (d_f) for each user in PD-NOMA;
- The optimization problem for equity power allocation is solved through an FIS-based system that guarantees user-fairness in terms of the optimal power distribution among PD-NOMA users;
- In realistic 5G micro-cells, the Weissberger model is being used to analyze the impact of foliage on channel conditions between the gNodeB and users;
- The proposed methodology employs the decode and forward (D&F) cooperation relaying mechanism at the cell-center level to improve BER performance at the cell-edge level, where a maximum ratio combining (MRC) is used for detection.

The rest of the paper is organized as follows. Section 2 presents the system model, optimal PA and cooperative relaying PD-NOMA is discussed in Section 3, respectively. Section 4 provides the simulation results. Finally, conclusions are drawn in Section 5.

2. System Model

An ideal 5G micro-cell with a coverage radius of 200 m is shown in Figure 1. This micro-cell consists of a gNodeB which serves two users U_1 (near-user) and U_2 (far-user), via downlink PD-NOMA communication. The gNodeB and two users (U_1 and U_2) are installed with single antennas. In the downlink PD-NOMA, the gNodeB is considered the controlling unit which allocates different powers to each serving user at the same time and frequency. The fuzzy inference system (FIS) based optimal PA strategy is used in the proposed methodology. To obtain user fairness, U_1 is given a minimum power and U_2 a maximum power, as demonstrated in Figure 1.

At the gNodeB, random symbol bits for the ith user are generated, which is given by:

$$r_i(t) = \sum_l b_i^l \delta(t - iT_s), \tag{1}$$

where $r_i(t)$ represents the randomly generated symbol bits and b_i^l is the ith user's lth symbol. δ and T_s represent the Dirac delta function and the sampling rates, respectively. For each user the absolute power factor is computed through FIS as shown in Section 3 and

Appendix A. The output of the FIS system is normalized to obtain the actual power factors for each user and is given by:

$$P_i = \frac{p_i^{'}}{\sum_{i=1}^{2} p_i^{'}}, \tag{2}$$

where P_i and $p_i^{'}$ are the normalized and absolute power factors for ith user, respectively. The total normalized power for all users is constrained by:

$$\sum_{i=1}^{2} P_i = 1. \tag{3}$$

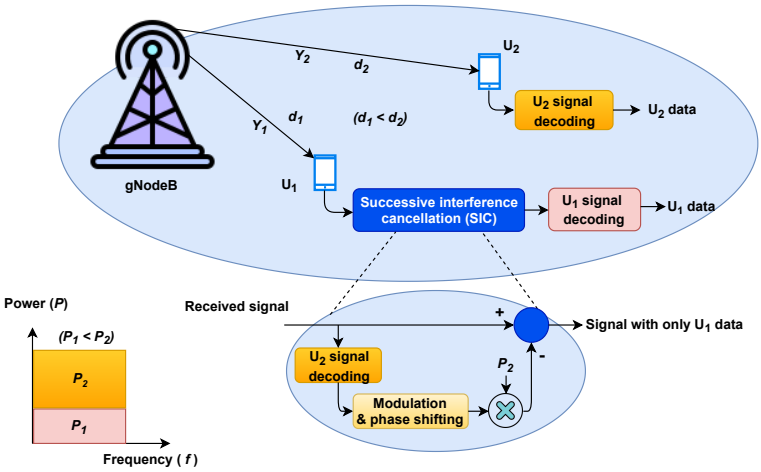

Figure 1. SISO downlink PD-NOMA system (U_1 is near-user and U_2 is far-user).

Each user's signal is modulated with Binary Phase Shift Keying (BPSK) along distinct phase offsets and assigned with corresponding power factors via FIS at the gNodeB, and is given by:

$$c_i(t) = \sqrt{P_i} r_i(t) = \sqrt{P_i} \sum_{l} b_i^{(l)} g(t - iT_s), \tag{4}$$

where $c_i(t)$ is the ith user's power multiplexed signal and $g(t)$ stands for the transmitting pulse. The combined signal for both users is given by:

$$x(t) = \sum_{i=1}^{2} \sqrt{P_i} c_i(t). \tag{5}$$

The combined signal $x(t)$ after passing through root raised cosine filter (RRCF) for pulse shaping is transmitted over a channel in the presence of additive white Gaussian noise (AWGN). Each user (U_i) obtains the transmitted combined signal after it has been subjected to large-scale fading and is given by:

$$Y_i(t) = \alpha_i x(t) + n_i(t), \tag{6}$$

where $Y_i(t)$ is the received combined signal at the ith receiver, α_i is the channel gain and $n_i(t)$ is the AWGN with zero mean and standard deviation σ. The message signal is decoded by each receiver based on power levels. Signals with higher multiplexed power are decoded first, followed by those with lower power levels in descending order. The far-user (U_2) will decode its signal immediately due to maximum power, whereas the near-user U_1 will conduct SIC to negate the influence of the U_2 signal and then decode its signal, which is provided by:

$$\hat{x_i}(t) = Y_i(t) - x_{i'}(t). \tag{7}$$

$\hat{x_i}(t)$ is the decoded signal and $x_{i'}(t)$ is the SIC term. Here, $i' = 2$ for near-user (U_1) and $i' = 1$ for far-user (U_2). The proposed framework is represented in Figure 2, which illustrates a step-by-step block diagram of the proposed framework, where each user signal is given different phase shifts and assigned the associated power factors by employing an FIS-based system. All of the users' signals are superimposed, then sent over the channel after passing through a root-raised cosine filter (RRCF) for pulse shaping. At the receiving end, the incoming signal is processed once more by RRCF before being decoded using the SIC technique. The near-user U_1 is used for cooperation to assist the far-user U_2 using the D&F technique, which is further discussed in Section 3.2.

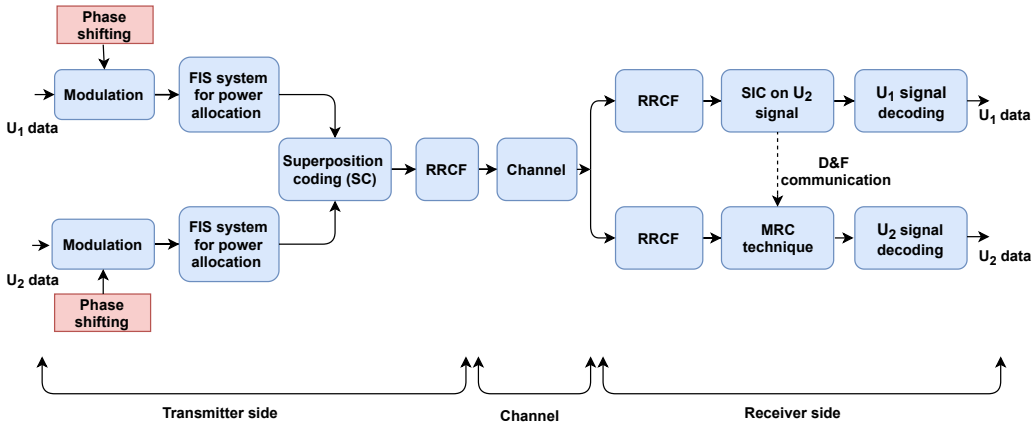

Figure 2. Block diagram of the proposed cooperative relaying FIS based PD-NOMA system.

3. Optimal Power Allocation (PA), Cooperative Relaying and Channel Models in PD-NOMA

3.1. Fuzzy Inference System for Optimal PA

In comparison to conventional logic systems, fuzzy logic is largely reliant on human reasoning in spirit and is considerably closer to natural language. The fuzzy logic controller mimics the actions of a human operator by modifying the input signal. The proposed technique uses an FIS-based system to address the issue of power allocation. Normally, in the downlink PD-NOMA users' signals are assigned different power levels at the gNodeB but this is not the optimum solution for practical implementation of the NOMA system. To solve this issue, we proposed an FIS-based optimization technique that effectively distributes the total power among all the user signals at the gNodeB. The FIS system uses a fuzzy rule-based system (FRBS) that takes different input variables and mimics them identically as humans perform. The power optimization problem is solved using the FIS system, which allocates an optimal power factor to each user surrounding the gNodeB. Fuzzy logic (FL) is relatively less complicated and simpler to configure the model for solving non-convex and multi-objective systems with greater efficiency [41]. A normal fuzzy system is composed of three different levels: fuzzification, rule base, and defuzzification. The input values are transformed to fuzzy values in the fuzzification stage. The output of the fuzzification stage is executed depending on the different fuzzy rules from the fuzzy rule matrix (FRM) in the rule base. The fuzzy results from the rule base are turned into final output values via defuzzification.

3.1.1. Selection of Fuzzy Sets

At this stage, the fuzzy inputs and their respective membership functions (MFs) are chosen to enfold the complete range of inputs and outputs. The FIS system takes different input signals at the gNodeB, such as d, SNR, and d_f for each serving user in its vicinity. Each input has three triangular MFs, which are labeled as low (L), moderate (M), and high (H). In the fuzzification stage, all three input variables are transformed into fuzzy values: μ_d, μ_{SNR} and μ_{d_f}. Our proposed FIS system is implemented for d = 200 m, SNR = 30 dB, and d_f = 30 m. However, if the universe of discourse changes, the same MF should be utilized

to cover the entire range of input parameters. The output function is also triangular and consists of five MFs: very low (VL), low (L), moderate (M), high (H), and very high (VH). All the three inputs and output MFs are shown in Figures 3–6, respectively. The triangular MFs are produced with min-max (and-or) operations [42] for implication/aggregation. With a high point (α, h) and end points $(e, 0)$ and $(f, 0)$, the triangular membership function $T(s)$ is given by:

$$T(s) = \begin{cases} h(\frac{s-e}{\alpha-e}) & \text{for} \quad e \leq s \leq \alpha \\ h(\frac{s-f}{\alpha-f}) & \text{for} \quad \alpha \leq s \leq f \\ 0 & \text{otherwise} \end{cases} . \tag{8}$$

Here, s is the input parameter such as d, SNR, and d_f.

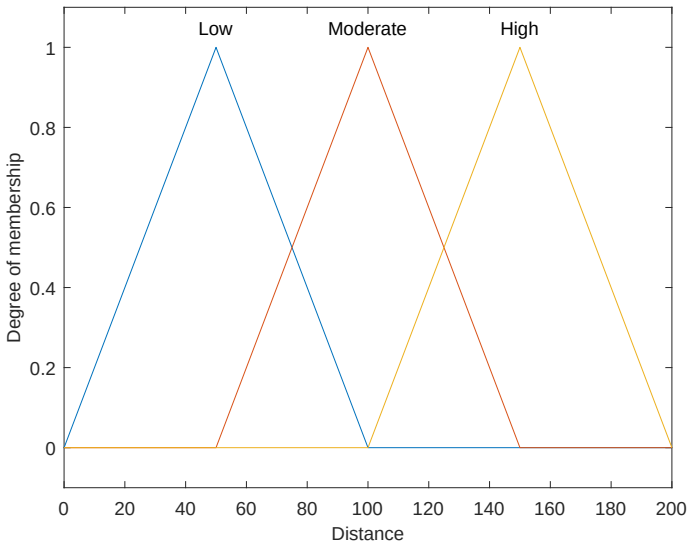

Figure 3. Membership function (MF) plot for input variable distance (d).

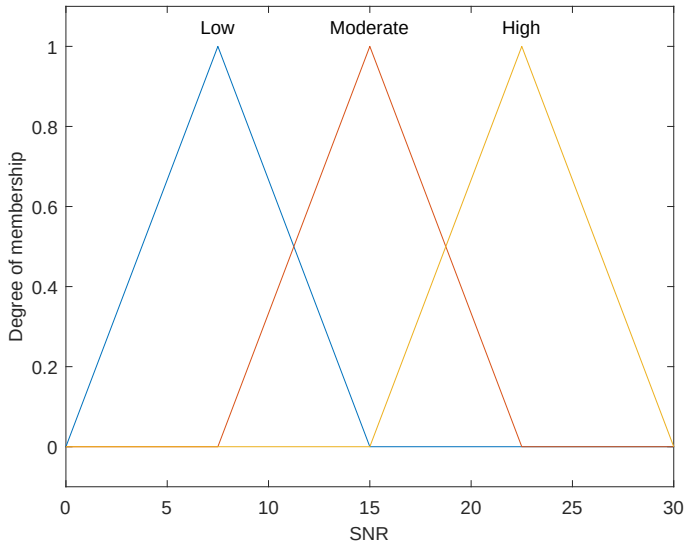

Figure 4. Membership function (MF) plot for input variable (SNR).

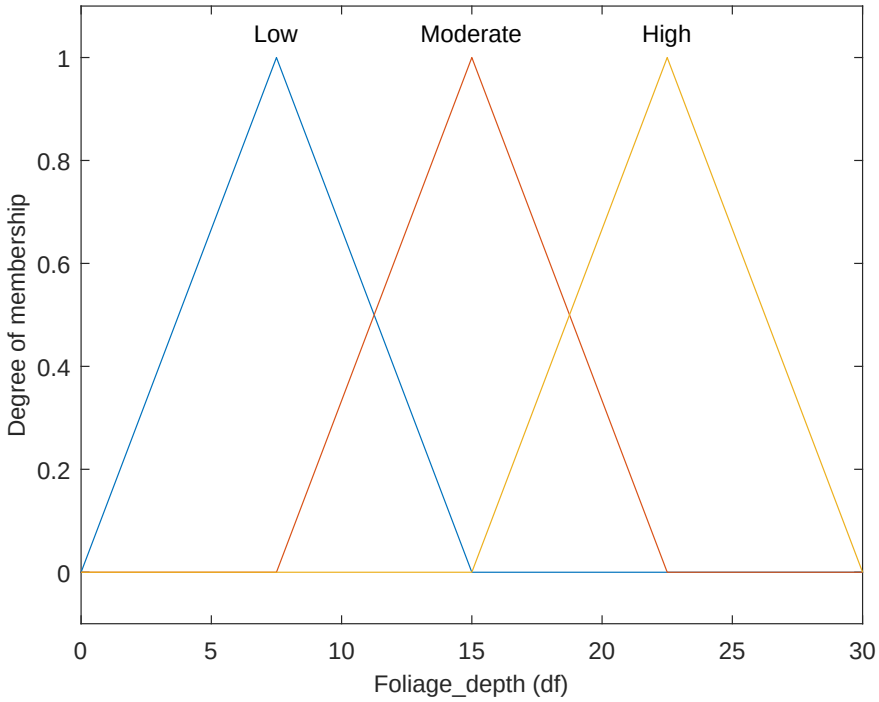

Figure 5. Membership function (MF) plot for input variable foliage depth (d_f).

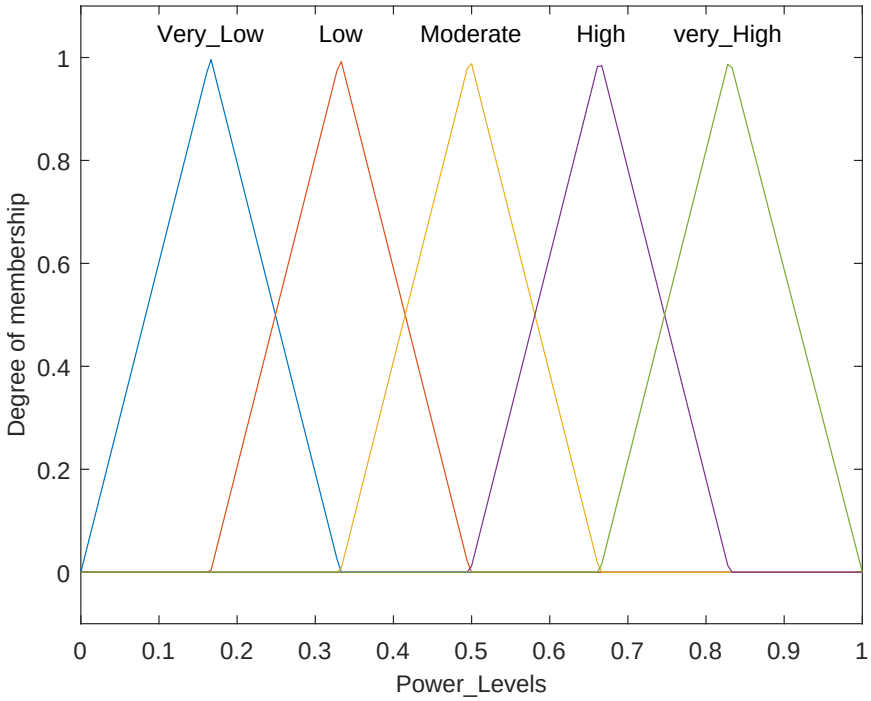

Figure 6. Membership function (MF) plot for output variable power levels.

3.1.2. Fuzzy Rule Matrix (FRM) for Optimal PA

The FRM is the decision-taking stage of the FIS system. At this stage, the output of the fuzzification stage is passed through the FRM for execution. The FRM depends on the input parameters and their respective MFs for each fuzzy value. It uses IF-THEN logical statements for the appropriate execution of fuzzy inputs. The proposed system gives more weight to the input variable SNR for each user signal. It means if SNR is low, comparatively more power will be allocated to that user. In other words, the impact of

input variable SNR on PA is comparatively greater than the other inputs, such as distance and foliage depth. The FRM is made up of 27 possible rule combinations based on the input variables and their respective MFs: $d = \{d_L, d_M, d_H\}$, $SNR = \{SNR_L, SNR_M, SNR_H\}$, and $d_f = \{df_L, df_M, df_H\}$. The FRM observes the fuzzy inputs and takes decisions, which are then used as inputs to the defuzzification stage. Table 1, depicts the fuzzy rule-based system for three inputs. To better understand the Table 1, we have three input variables, d, SNR, and d_f each consisting of three different triangular MFs: L, M, and H. So a combination of 27 different rules are implemented using these input variables. The outcome of the FIS-based system has five MFs (VL, L, M, H, and VH), that are completely dependent on the arrangements of input parameters: d, SNR, and d_f.

3.1.3. Defuzzification

In the defuzzification, the center of area (COA) technique [42] is used to calculate the optimal power factors using the proposed FRBS system. For various numbers of fuzzy rules, the defuzzifier's output is obtained by:

$$p_i^{'} = \frac{\sum_i \mu_{Ci}(\Delta\mu)\Delta\mu(Ci)}{\sum_i \Delta\mu(Ci)}. \tag{9}$$

For the rule Ci, $\Delta\mu(Ci)$ specifies the peak value of the fuzzy set's membership degree and μ_{Ci} represents the centroid of the associated output membership function. Using Equation (9), each user is assigned an absolute power factor based on the FRM, which is then normalized through Equation (2) to produce real power factors. Figure 7 shows the graphical representation of the FIS system's output as a function of d and SNR. The foliage depth is kept constant at d_f = 14 m for a 3D graphical view. The output power factors for input d, SNR, and d_f are maximum for combinations (H, L, H) and minimum for combinations (L, H, L). For a better understanding of Table 1 in terms of the FIS system's outcome for the different power levels, we assumed the input arrangements for row 21 (H, L, and H). The FIS system will result in maximum power levels for each user if the distance is high (H), the SNR is low (L), and the foliage depth is high (H). The same intuition is tabulated for all the power levels calculated.

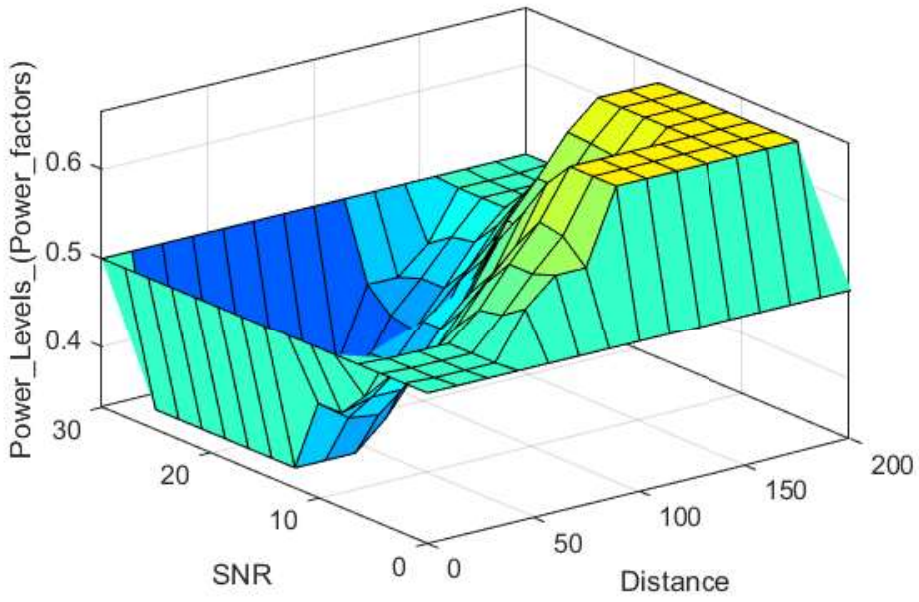

Figure 7. Graphical view of the FIS system's output.

Table 1. Human Intuition based FIS system for Optimal PA in PD-NOMA.

S.no	d	SNR	d_f	Power Level
1	L	L	L	L
2	L	L	M	M
3	L	L	H	H
4	L	M	L	L
5	L	M	M	L
6	L	M	H	M
7	L	H	L	VL
8	L	H	M	L
9	L	H	H	L
10	M	L	L	M
11	M	L	M	H
12	M	L	H	H
13	M	M	L	L
14	M	M	M	M
15	M	M	H	H
16	M	H	L	L
17	M	H	M	L
18	M	H	H	M
19	H	L	L	H
20	H	L	M	H
21	H	L	H	VH
22	H	M	L	M
23	H	M	M	H
24	H	M	H	H
25	H	H	L	L
26	H	H	M	M
27	H	H	H	H

3.2. Cooperative Relaying and Channel Models in PD-NOMA

In cooperative relaying communication, the strong node is used as a relay to assist the weak node in the system. A strong node has better channel conditions than a weak node. In the proposed model, the strong and weak nodes are U_1 and U_2, respectively, as shown in Figure 8. The weak node faces critical signal losses due to multiple issues such as greater distance separation, foliage depth, and low signal-to-noise ratio. Although PD-NOMA assigns higher power to far users' signals to ensure user fairness, it is further needed to assist them from strong nodes as well, which provide indirect line-of-sight (LOS) paths between the gNodeB and the far-users (U_2 here).

In Figure 8, U_2 being located at a maximum distance and foliage depth faces signal degradation and results in intense path losses. To address this issue that occurs in ordinary PD-NOMA, the proposed model incorporates cooperative relaying into the existing system by treating U_1 as a relay that uses the decode and forward (D&F) method to assist U_2. Specifically, during the time slot (t_1), both users U_1 and U_2 receives the combined signal. The U_1 first decodes the U_2 signal using basic NOMA principles and performs SIC on the U_2 signal to retrieve its signal. The U_2 signal is regenerated from the previously decoded

signal at U_1 and forwarded to the U_2 receiver at time slot (t_2). Cooperation in the system can be implemented at the expense of increased bandwidth consumption. Now U_2 has two signals: a degraded signal from the gNodeB with higher path losses and a D&F signal from node U_1. The maximum ratio combining (MRC) technique is then used by the U_2 receiver to decode its signal.

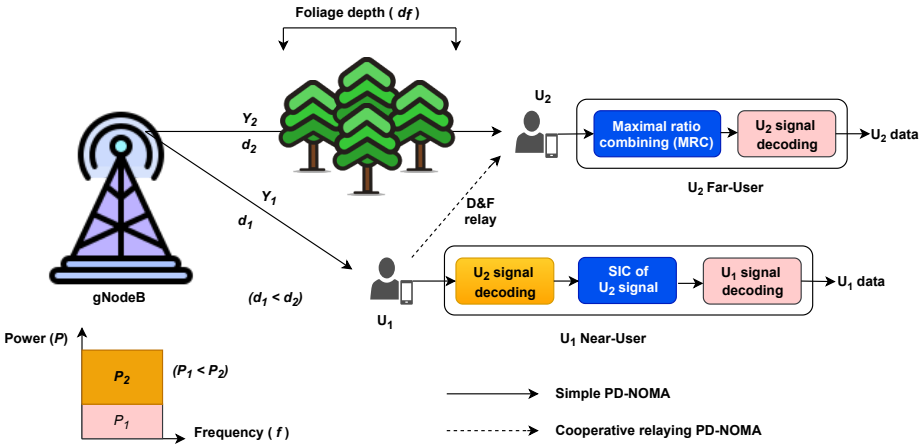

Figure 8. SISO cooperative relaying PD-NOMA model (U_1 is used as a relay).

We used three types of channel models: NYUSIM, Rician, and Rayleigh channels, to study the behavior of the proposed model. The NYUSIM [43] channel model, which was created specifically for 5G wireless communication protocols and covers a frequency range of 500 MHz to 100 GHz. The path loss (PL) calculated for each user signal by passing it through the NYUSIM channel model is given by:

$$\mathrm{PL}(f_c, d)[\mathrm{dB}] = \mathrm{FSPL}(f_c, 1\ \mathrm{m})[\mathrm{dB}] + 10n\log_{10}(d/d_0) + \mathrm{AT}[\mathrm{dB}] + X_\sigma. \tag{10}$$

f_c is the carrier frequency in gigahertz and d is the 3D distance between each user and the gNodeB. d_o is the reference distance of 1 m, n denotes the path loss exponent, and AT denotes the attenuation effect from the surrounding environment. X_σ represents a Gaussian random variable with zero mean and a variance of 2.52. The free space path loss (FSPL) in Equation (10) is given by:

$$\begin{aligned} \mathrm{FSPL}(f_c, 1\ \mathrm{m})[\mathrm{dB}] &= 20\log_{10}\left(\frac{4\pi \times f_c \times 10^9}{c}\right) \\ &= 32.4[\mathrm{dB}] + 20\log_{10}(f_c), \end{aligned} \tag{11}$$

where, c denotes speed of light. The 3-D distance separation is given by:

$$d = \sqrt{d_{2D}^2 + (h_t - h_r)^2}, \tag{12}$$

where d_{2D} denotes the 2-D distance separation for each user from the gNodeB, h_t and h_r are the gNodeB and each user heights, respectively. The environment attenuation is given by:

$$\mathrm{AT}[\mathrm{dB}] = \beta[\mathrm{dB/m}] \times d[\mathrm{m}]. \tag{13}$$

Here, β represents the factor of attenuation from the surrounding environment and d[m] is the 3D distance separation. The proposed model is also simulated in the Rician and Rayleigh fading channels. In the Rician fading channel, the SUI-3 (Stanford University Interm channel model 3) parameters are used in the simulation. The K-factor (line of sight paths) is equal to 1, the path delay vector is [0 0.4 0.9], the path gain vector in dB is [0 −5 −10], and a doppler spread equal to 0.5 is chosen. For the Rayleigh fading channel,

SUI-6 parameters are used, such as K-factor equal to 0, path delay vector is [0 14 20], path gain vector in dB is [0 −10 −14], and a doppler spread equal to 0.5.

In practical scenarios, the 5G micro-cell may consist of plants or foliage. This foliage drastically affects high-frequency communications, such as mm-Wave communication at GHz frequencies. The losses are proportional to the foliage depths (d_f) and carrier frequency. In the proposed model, we use the ITU-developed Weissberger model [44,45], which accounts for propagation losses related to foliage.

$$PL_{d_f} = \begin{cases} 1.33 f_c^{0.284} d_f^{0.588}, & 14m < d_f \leq 400m \\ 0.45 f_c^{0.284} d_f, & 0m < d_f \leq 14m \\ , \end{cases} \tag{14}$$

where PL_{d_f} denotes the path loss due to foliage, f denotes the frequency in GHz and d_f is the foliage depth. We simulate the Weissberger model at 28 GHz with different foliage depths as shown in Figure 9. As the foliage distance between the BS and the user increases, the path loss increases as well, as shown in Figure 9. So it is recommended that for larger foliage depths among the gNodeB and users, higher power will be assigned to those users.

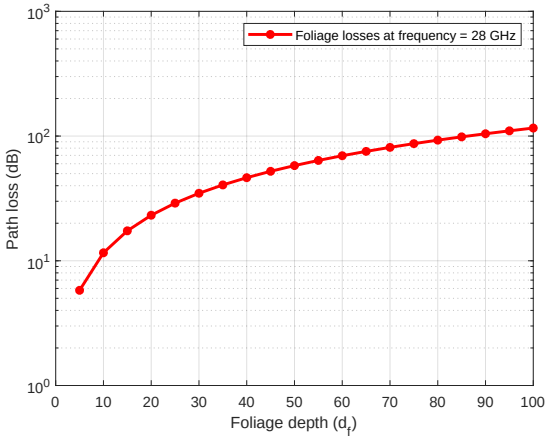

Figure 9. Path losses calculated through ITU developed Weissberger model.

The total path losses for a user are calculated by adding NYUSIM path losses (PL(f_c, d)) and foliage losses (PL$_{d_f}$) which is given by:

$$\text{PL}_{total} = \text{PL}(f_c, d) + \text{PL}_{d_f}. \tag{15}$$

In the results section, we conclude from Figures 10 and 11, that incorporating the cooperative relaying technique into ordinary PD-NOMA systems improves the BER performance of U_2.

4. Simulation Results

In this section, the proposed system's simulation results are discussed in detail. A frequency of 28GHz is employed as the operational frequency. The system is implemented for two users (U_1 & U_2) in SISO downlink cooperative relaying PD-NOMA with different pairs of optimal powers. The FIS system is used to allocate these powers (optimal power factors). Table 2 lists the parameters utilized in the simulation model. The coverage radius of the gNodeB is set to 200 m, which is ideal for 5G BS (gNodeB). For simplicity, single antennas are installed on both the gNodeB and the users (U_i) sides. The heights of the gNodeB and the users have been set to 10 m and 1 m, respectively. The path loss exponent is set to 2, which is the standard value for the free space, and the modulation scheme of BPSK is used to avoid large interference issues. The proposed FIS system is compared based on optimal PA and user fairness. For comparison analysis, the proposed method simulates

the existing the existing DBPA algorithm from [18] for two users in the PD-NOMA system. The FIS system is then utilized to assign optimal power to each user, and the two power distribution strategies are compared in terms of performance. The bit-error-rate (BER) for each user signal is calculated using Monte Carlo simulations to determine the difference between transmitted and received bits. The BER curves at 10^{-3} along the Y-axis are used to compare the results, and hence they are plotted against different SNR values.

Table 2. Parameters used in implementation of System Model.

Parameters	Values
Carrier frequency (f_c)	28 GHz
gNodeB radius	200 m
gNodeB and U_i antenna	(SISO) 1,1
gNodeB height (h_t)	10 m
β	0.0019 (Collective)
Users (U_i) height (h_r)	1 m
Path Loss exponent (n)	2
Modulation schemes	BPSK
Phase shifts	$\pi/2, 0$
X_σ	Mean 0, variance 2.52

The comparison of BER curves for PD-NOMA employing DBPA and the proposed FIS-based optimal PA schemes is shown in Figure 10. The distance separation of near-user U_1 and far-user U_2 from gNodeB is $d_1 = 60$ m and $d_2 = 180$ m, respectively. Using the DBPA scheme, U_1 is allocated with $P_1 = 0.23$ and U_2 with $P_2 = 0.77$. The FIS system uses three parameters to determine optimal powers for each user: (d_1 = 60 m, d_{f1} = 10 m and SNR_1 = 14 dB) for user U_1 and (d_2 = 180 m, d_{f2} = 28 m and SNR_2 = 10 dB) for user U_2. Here, $P_1 = 0.34$ and $P_2 = 0.66$ are the calculated power factors for users U_1 and U_2, respectively. The FIS system ensures fairness by providing optimal powers with equity. Fairness can be seen from the obtained SNR levels at a threshold BER of 10^{-3}. The proposed methodology integrates D&F cooperation in addition to assigning optimal powers. Due to the D&F cooperation scheme implemented at the near-user level U_1 helps to enhance the performance of far-users U_2. Using DBPA scheme, the obtained SNR levels at a threshold BER is 10 dB for user U_1 and 5 dB for user U_2, subsequently. While using the FIS system, the obtained SNR levels are: U_1 at 8.8 dB; U_2 at 7 dB (in only PD-NOMA), and 6 dB (in D&F PD-NOMA). In the case of DBPA scheme, the difference between the obtained SNR levels is 5 dB, while it is only 2.8 dB in the FIS-based system. In this context, the largest SNR difference in DBPA scheme indicates that powers are not distributed fairly, whereas the minimal SNR level in the FIS-based system establishes justice between users in terms of PA. Similarly, another attempt was made to test and compare the proposed FIS-based methodology with the DBPA scheme in Figure 11, for distinct input signals. Here in DBPA scheme, U_1 with d_1 = 40 m is assigned with P_1 = 0.32 and U_2 with d_2 = 80 m is allocated with P_2 = 0.68. As a result, U_2 obtains an SNR of 5.4 dB and U_1 obtains an SNR of 9 dB. So, the obtained SNR difference between the users is 3.6 dB. On the other hand, the FIS-based system uses (d_1=40 m, d_{f1} = 5 m, and SNR_1 = 15 dB) and (d_2=80 m, d_{f2} = 10 m, and SNR_2 = 10 dB) for U_1 and U_2, subsequently. Here, the FIS system results in P_1 = 0.44 and P_2 = 0.56. The obtained SNR level is 8 dB for U_1; 6.3 dB and 6.6 dB for U_2 with D&F cooperation and only PD-NOMA, respectively. Here, the highest SNR difference is 1.7 dB, which indicates that power is fairly distributed among users and hence user fairness is established.

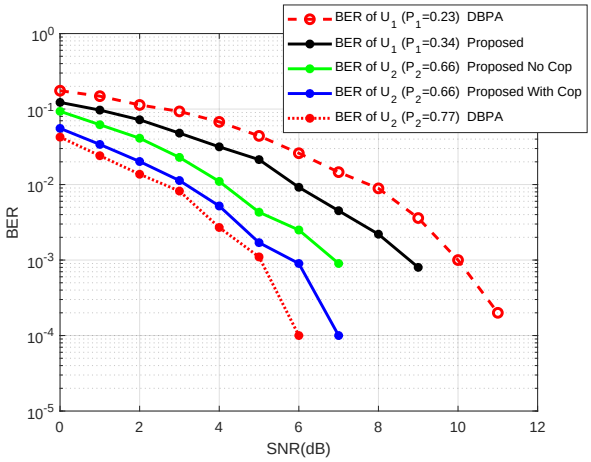

Figure 10. Comparisons of BER performance for 2 users, in DBPA scheme [18] and the proposed FIS based model.

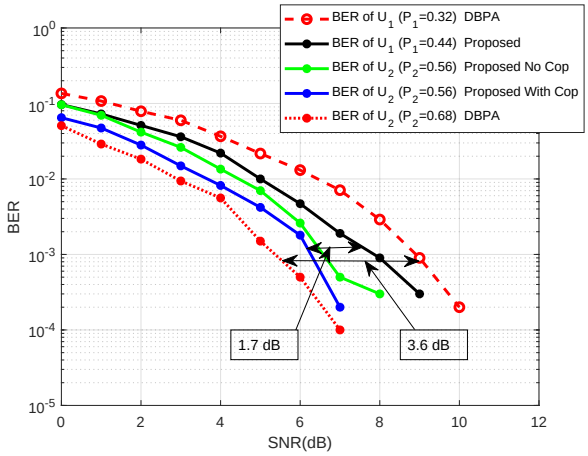

Figure 11. Comparisons of user fairness, in DBPA scheme [18] and the proposed FIS based model for two users in terms of the difference between obtained SNR levels.

Furthermore, simulation is carried out for the proposed FIS-based model in the Rician and Rayleigh channels. The SUI-3 and SUI-6 models are utilized as standard parameter values for Rician and Rayleigh fading channels, respectively. The BER performance for the proposed FIS-based system is compared with the DBPA in Figures 12 and 13 under the Rician and Rayleigh fading channels, respectively. Similar to previous results from NYUSIM models, the proposed technique again outperforms under these two channels in terms of user-fairness. In the Rician channel, the proposed FIS-based system achieves a threshold BER of 10^{-3} at an SNR of 11.4 dB for U_1 ($P_1 = 0.34$); 8.2 dB and 8.4 dB for U_2 ($P_2 = 0.66$) with D&F cooperation and only PD-NOMA, respectively. While utilizing the DBPA scheme, the threshold BER is achieved at SNRs of 13.2 dB for U_1 and 8 dB for U_2, respectively. The DBPA allocates $P_1 = 0.23$ to U_1 and $P_2 = 0.77$ to U_2, respectively. Here, again, we can see the difference in the achieved SNRs between U_1 and U_2 is less in the case of the proposed FIS-based than the DBPA. As we can see in Figure 12 the SNR difference in FIS-based is 3.2 dB while it is 5.2 dB for DBPA. Similarly, Figure 13 also ensures that an FIS-based system outperforms the DBPA schemes in terms of optimal power allocation and user-fairness. The lower the difference between the achieved SNR levels, the larger the user-fairness and vice versa. User-fairness is the key capability of the NOMA technique that differentiates it from other OMA techniques. In comparison with the power allocation scheme of DBPA, the proposed FIS-based allocates optimal power factors with equity and fair-play and hence ensures user-fairness. The BER performance when utilizing the Rician channel is comparatively better than that of the Rayleigh channel. This is because the Rician

channel has more line-of-sight (LOS) paths (K-factor) than the Rayleigh channel, which has no LOS paths and more delays.

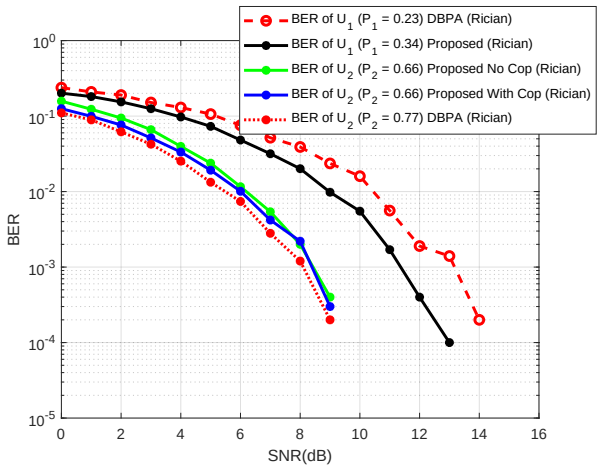

Figure 12. BER performance for two users, in the proposed FIS based model in Rician (SUI-3) Channel Model.

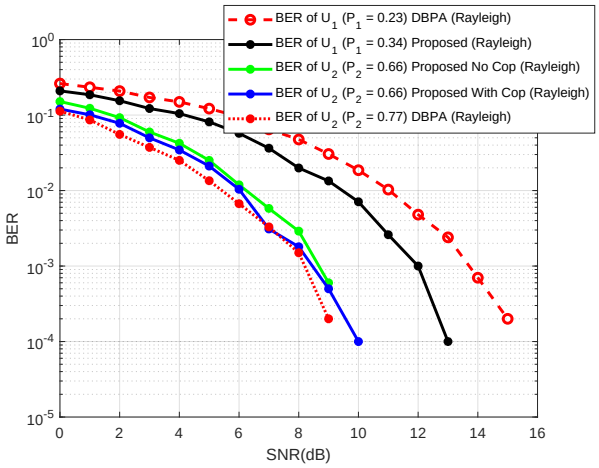

Figure 13. BER performance for two users, in the proposed FIS based model in Rayleigh (SUI-6) Channel Model.

In the DBPA scheme, the far-user is allocated higher power and the near-user with lower power, but this is the case when power is distributed among users based on distance separation from the gNodeB. However, the proposed FIS system decides the PA based on multi-input parameters. Given the foregoing, it is possible that, despite being close to the gNodeB, a near-user (U_1) has poor channel condition due to low input SNR and high foliage depth, as compared to a far-user (U_2) having high input SNR and low foliage depth. In this case, the proposed FIS system assigns maximum power to U_1 and minimum power to U_2. The simulation is performed for a scenario in which U_1 has (d_1 = 90 m, SNR_1 = 15 dB, and df_1 = 25 m) and U_2 has (d_2 = 110 m, SNR_2 = 25 dB, and df_2 = 8 m) from the gNodeB. The FIS-based system assigns optimal power factors of P_1 = 0.64 and P_2 = 0.36 to U_1 and U_2, respectively. In this case, U_1 will not be used as a relay node to assist the far-user U_2. The reason is simple: U_1 suffers from greater signal losses due to low input SNR and high foliage depth, and hence its contribution as a relay node is negligible. It is observed that U_1, which is closer to gNodeB and has higher power, directly decodes its signal from the combined signal, whereas U_2, which is further away and has a lower power factor, uses the SIC technique to negate the effect of the U_1 signal from the combined signal to retrieve its U_2 signal. As shown in Figure 14, the BER threshold of 10^{-3} is obtained at an SNR of 6 dB and 8 dB by U_1 and U_2, respectively. The degraded U_2 performance is caused by

using the SIC technique on the U_1 signal. Table 3 contains a detailed description of the parameters and the results obtained in various attempts. The complexity of the FIS system increases with the number of inputs and outputs, the number of MFs used for the universe of discourse, and the selection of different rule base sets.

Table 3. Performance analysis of two users in PD-NOMA and Cooperative PD-NOMA with PA through DBPA and the FIS-based strategies.

Users	d	i/p SNR	d_f	Power Factor (DBPA)	Power Factor (FIS)	SNR Level Obtained (DBPA)	SNR Level Obtained (FIS)
UE_1	60 m	14 dB	10 m	0.23	0.34	10 dB	8.8 dB
UE_2	180 m	10 dB	28 m	0.77	0.66	5 dB	6 dB (with D&F), 7 dB (No D&F)
UE_1	40 m	15 dB	5 m	0.32	0.44	9 dB	8 dB
UE_2	80 m	10 dB	10 m	0.68	0.56	5.4 dB	6.3 dB (with D&F), 6.6 dB (No D&F)
UE_1	90 m	15 dB	25 m	–	0.64	–	6 dB
UE_2	110 m	25 dB	8 m	–	0.36	–	8 dB (No D&F)

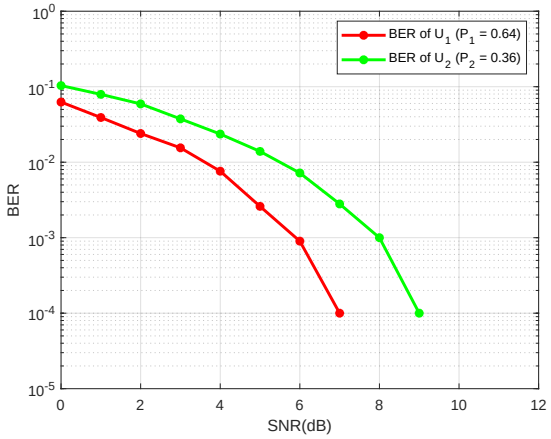

Figure 14. Performance analysis for two users in the proposed FIS based system where U_1 is assigned a maximum power factor and U_2 a minimum power factor.

5. Conclusions

Key aspects of power domain NOMA (PD-NOMA) and cooperative relaying PD-NOMA are successfully presented in this study. An FIS-based system is used to precisely address the power optimization problem, which is a fundamental aspect of PD-NOMA. The proposed system evaluates the performance of PD-NOMA in a scenario where mmWave signals are degraded around the gNodeB. Overall, the proposed system achieves user-fairness, and system performance is considerably improved thanks to FIS-based power optimization and cooperative relaying. Future studies on the proposed technique can include multiuser clustering systems with multiple cooperation stations, allowing multiple cell-center users to cooperate with the cell-edge users for performance improvement in denser PD-NOMA networks.

Author Contributions: Conceptualization, A.M., M.M. and M.Z.; formal analysis, M.M. and M.M.N.; data curation, A.M. and M.A.E.; investigation, A.M. and M.M.; methodology, A.M. and M.Z.; project administration, M.M.; supervision, M.M., M.Z., M.M.N. and M.A.E.; validation, A.M.; writing—original draft, A.M.; writing—review and editing, M.M., M.M.N. and M.A.E. All authors have read and agreed to the published version of the manuscript.

Funding: The Article Processing Charges (APC) was funded by Prince Sultan University.

Acknowledgments: The authors would like to acknowledge the support of Prince Sultan University for paying the Article Processing Charges (APC) for this publication.

Conflicts of Interest: The authors declare no conflict of interest.

Appendix A. Numerical Example for the Proposed FIS-Based System

Equation (14) and (15), are used for the numerical example of the proposed FIS-based system. The multi-input signals for users U_1 and U_2 are (d_1 = 60 m, SNR_1 = 14 dB, and d_{f1} = 10 m) and (d_2 = 180 m, SNR_2 = 10 dB, and d_{f2} = 28 m), respectively. For user U_1 the fuzzy values are calculated by,

$$T(s) = \begin{cases} h(\frac{s-e}{\alpha-e}) & \text{for} \quad e \leq s \leq \alpha \\ h(\frac{s-f}{\alpha-f}) & \text{for} \quad \alpha \leq s \leq f \\ 0 & \text{otherwise} \end{cases} \tag{A1}$$

For d_1 = 60 it touches two triangular MFs (L and M), refer to Figure 3. For L it uses second part of the equation. Here s = 60, h = 1, α = 50, and f = 100. Then $T_L(60)$ = 0.6666. For M it uses first part of the equation. Here s = 60, h = 1, α = 100, and e = 50. Then $T_M(60)$ = 0.2.

For SNR_1 = 14 dB again it touches the two MFs (L and M), refer to Figure 4. For L, s = 14, h = 1, α = 7.5, e = 0, and f = 15, using the second part of . Then $T_L(14)$ = 0.1333. For M, s = 14, h = 1, α = 15, e = 7.5 and f = 22.5. Then $T_M(14)$ = 0.8666.

Similarly, for d_{f1} = 10 m the L MF has s = 10, h = 1, α = 7.5, e = 0, and f = 15. Then $T_L(10)$ = 0.6666. When d_{f1} is M then s = 14, h = 1, α = 15, e = 7.5 and f = 22.5. Then $T_M(10)$ = 0.3333.

From Table 1 the possible rule combination for the multi-input variables are calculated through rule base stage which uses AND operation to create fuzzy outputs which are,

- $\Delta\mu(C_1)$ = min (0.6666, 0.1333, 0.6666) = 0.1333, and μ_{C_1} = 0.3332.
- $\Delta\mu(C_2)$ = min (0.6666, 0.1333, 0.3333) = 0.1333, and μ_{C_2} = 0.4998.
- $\Delta\mu(C_3)$ = min (0.6666, 0.8666, 0.6666) = 0.6666, and μ_{C_3} = 0.3332.
- $\Delta\mu(C_4)$ = min (0.6666, 0.8666, 0.3333) = 0.3333, and μ_{C_4} = 0.3332.
- $\Delta\mu(C_5)$ = min (0.2, 0.1333, 0.6666) = 0.1333, and μ_{C_5} = 0.4998.
- $\Delta\mu(C_6)$ = min (0.2, 0.1333, 0.3333) = 0.1333, and μ_{C_6} = 0.6664.
- $\Delta\mu(C_7)$ = min (0.2, 0.8666, 0.6666) = 0.2, and μ_{C_7} = 0.3332.
- $\Delta\mu(C_8)$ = min (0.2, 0.8666, 0.3333) = 0.2, and μ_{C_1} = 0.4998.

Here $\Delta\mu_{C_i}$ is the corresponding fuzzy outputs for rule C_i which is the FRBS rules combination as shown in Table 1. μ_{C_i} is the centroid of respective MF in Figure 6. By putting the values in Equation (15) it gives the output power factor $p_1^{'}$ = 0.383.

The same is repeated for user U_2 with multi-input signal (d_2 = 180 m, SNR_2 = 10 dB, and d_{f2} = 28 m). The output power factor is $p_2^{'}$ = 0.749. Both the power factors are normalized to obtain the actual power factors P_1 and P_2, respectively, using Equation (2). The normalized power factors are P_1 = 0.34, and P_2 = 0.66, respectively.

References

1. Saito, Y.; Kishiyama, Y.; Benjebbour, A.; Nakamura, T.; Li, A.; Higuchi, K. Non-orthogonal multiple access (NOMA) for cellular future radio access. In Proceedings of the 2013 IEEE 77th Vehicular Technology Conference (VTC Spring), Dresden, Germany, 2–5 June 2013; pp. 1–5.
2. Makki, B.; Chitti, K.; Behravan, A.; Alouini, M.S. A survey of NOMA: Current status and open research challenges. *IEEE Open J. Commun. Soc.* **2020**, *1*, 179–189. [CrossRef]
3. Higuchi, K.; Benjebbour, A. Non-orthogonal multiple access (NOMA) with successive interference cancellation for future radio access. *IEICE Trans. Commun.* **2015**, *98*, 403–414. [CrossRef]
4. Ping, L.; Liu, L.; Wu, K.; Leung, W.K. Interleave division multiple-access. *IEEE Trans. Wirel. Commun.* **2006**, *5*, 938–947. [CrossRef]
5. Ping, L.; Wang, P.; Wang, X. Recent progress in interleave-division multiple-access (IDMA). In Proceedings of the MILCOM 2007-IEEE Military Communications Conference, Orlando, FL, USA, 29–31 October 2007; pp. 1–7.
6. Nikopour, H.; Baligh, H. Sparse code multiple access. In Proceedings of the 2013 IEEE 24th Annual International Symposium on Personal, Indoor, and Mobile Radio Communications (PIMRC), London, UK, 8–11 September 2013; pp. 332–336.
7. Al-Imari, M.; Imran, M.A. Low density spreading multiple access. In *Multiple Access Techniques for 5G Wireless Networks and Beyond*; Springer: Cham, Switzerland, 2019; pp. 493–514.
8. Chen, S.; Ren, B.; Gao, Q.; Kang, S.; Sun, S.; Niu, K. Pattern division multiple access—A novel nonorthogonal multiple access for fifth-generation radio networks. *IEEE Trans. Veh. Technol.* **2016**, *66*, 3185–3196. [CrossRef]
9. Larsson, E.G.; Edfors, O.; Tufvesson, F.; Marzetta, T.L. Massive MIMO for next generation wireless systems. *IEEE Commun. Mag.* **2014**, *52*, 186–195. [CrossRef]
10. Zeng, M.; Hao, W.; Dobre, O.A.; Ding, Z. Cooperative NOMA: State of the art, key techniques, and open challenges. *IEEE Netw.* **2020**, *34*, 205–211. [CrossRef]
11. Kryukov, Y.V.; Pokamestov, D.A.; Rogozhnikov, E.V.; Demidov, A.Y.; Gromova, Y.S. Experimental research of PD/NOMA. In Proceedings of the 2018 19th International Conference of Young Specialists on Micro/Nanotechnologies and Electron Devices (EDM), Erlagol, Russia, 29 June–3 July 2018; pp. 176–179.
12. Zhang, X.; Haenggi, M. The performance of successive interference cancellation in random wireless networks. *IEEE Trans. Inf. Theory* **2014**, *60*, 6368–6388. [CrossRef]
13. Ding, Z.; Schober, R.; Poor, H.V. Unveiling the importance of SIC in NOMA systems—Part 1: State of the art and recent findings. *IEEE Commun. Lett.* **2020**, *24*, 2373–2377. [CrossRef]
14. Kang, J.M.; Kim, I.M. Optimal user grouping for downlink NOMA. *IEEE Wirel. Commun. Lett.* **2018**, *7*, 724–727. [CrossRef]
15. Lei, H.; Gao, R.; Park, K.H.; Ansari, I.S.; Kim, K.J.; Alouini, M.S. On secure downlink NOMA systems with outage constraint. *IEEE Trans. Commun.* **2020**, *68*, 7824–7836. [CrossRef]
16. Mahmood, A.; Zeeshan, M. Power allocation and performance analysis of multiuser NOMA under NYUSIM channel model. In Proceedings of the 2019 14th Conference on Industrial and Information Systems (ICIIS), Kandy, Sri Lanka, 18–20 December 2019; pp. 296–301.
17. Mahmood, A.; Khan, S.; Hussain, S.; Zeeshan, M. Performance Analysis of Multi-User Downlink PD-NOMA Under SUI Fading Channel Models. *IEEE Access* **2021**, *9*, 52851–52859. [CrossRef]
18. Mahmood, A.; Zeeshan, M.; Ashraf, T. A new hybrid CDMA-NOMA scheme with power allocation and user clustering for capacity improvement. *Telecommun. Syst.* **2021**, *78*, 225–237. [CrossRef]
19. Ali, S.; Hossain, E.; Kim, D.I. Non-orthogonal multiple access (NOMA) for downlink multiuser MIMO systems: User clustering, beamforming, and power allocation. *IEEE Access* **2016**, *5*, 565–577. [CrossRef]
20. Rihan, M.; Huang, L.; Zhang, P. Joint interference alignment and power allocation for NOMA-based multi-user MIMO systems. *EURASIP J. Wirel. Commun. Netw.* **2018**, *1*, 217. [CrossRef]
21. Khan, S.K.; Farasat, M.; Naseem, U.; Ali, F. Performance evaluation of next-generation wireless (5G) UAV relay. *Wirel. Pers. Commun.* **2020**, *113*, 945–960. [CrossRef]
22. Di Renzo, M.; Zappone, A.; Debbah, M.; Alouini, M.S.; Yuen, C.; De Rosny, J.; Tretyakov, S. Smart radio environments empowered by reconfigurable intelligent surfaces: How it works, state of research, and the road ahead. *IEEE J. Sel. Areas Commun.* **2020**, *38*, 2450–2525. [CrossRef]
23. Liu, Y.; Liu, X.; Mu, X.; Hou, T.; Xu, J.; Di Renzo, M.; Al-Dhahir, N. Reconfigurable intelligent surfaces: Principles and opportunities. *IEEE Commun. Surv. Tutor.* **2021**, *23*, 1546–1577. [CrossRef]
24. Liaqat, M.; Noordin, K.A.; Abdul Latef, T.; Dimyati, K. Power-domain non orthogonal multiple access (PD-NOMA) in cooperative networks: An overview. *Wirel. Netw.* **2020**, *26*, 181–203. [CrossRef]
25. Basar, E.; Di Renzo, M.; De Rosny, J.; Debbah, M.; Alouini, M.S.; Zhang, R. Wireless communications through reconfigurable intelligent surfaces. *IEEE Access* **2019**, *7*, 116753–116773. [CrossRef]
26. He, D.; Ai, B.; Guan, K.; Wang, L.; Zhong, Z.; Kürner, T. The design and applications of high-performance ray-tracing simulation platform for 5G and beyond wireless communications: A tutorial. *IEEE Commun. Surv. Tutor.* **2018**, *21*, 10–27. [CrossRef]
27. Glassner, A.S. (Ed.) *An Introduction to Ray Tracing*; Morgan Kaufmann: San Francisco, CA, USA, 1989.
28. Chen, Y.; Li, Y.; Han, C.; Yu, Z.; Wang, G.; Channel measurement and ray-tracing-statistical hybrid modeling for low-terahertz indoor communications. *IEEE Trans. Wirel. Commun.* **2021**, *20*, 8163–8176. [CrossRef]

29. Tian, Y.; Pan, G.; Alouini, M.S. On NOMA-based mmWave communications. *IEEE Trans. Veh. Technol.* **2020**, *69*, 15398–15411. [CrossRef]
30. Taj, N.; Zafar, M.H.; Waqas, S.A.; Rehman, H.; Alassafi, M.O.; Khan, I. Smart Relay Selection Scheme Based on Fuzzy Logic with Optimal Power Allocation and Adaptive Data Rate Assignment. *Int. J. Commun. Netw. Inf. Secur.* **2019**, *11*, 239–247.
31. Selvachandran, G.; Quek, S.G.; Lan, L.T.H.; Son, L.H.; Giang, N.L.; Ding, W.; Abdel-Basset, M.; Albuquerque, V.H.C. A new design of mamdani complex fuzzy inference system for multiattribute decision making problems. *IEEE Trans. Fuzzy Syst.* **2021**, *29*, 716–730. [CrossRef]
32. Diaz, J.L.; Mendel, J.M.; Junior, R.H. Fuzzy-System Kernel Machines: A Kernel Method Based on the Connections Between Fuzzy Inference Systems and Kernel Machines. *IEEE Trans. Fuzzy Syst.* **2022**, 1. [CrossRef]
33. Baldo, N.; Zorzi, M. Cognitive network access using fuzzy decision making. *IEEE Trans. Wirel. Commun.* **2009**, *8*, 3523–3535. [CrossRef]
34. Joshi, G.P.; Acharya, S.; Kim, S.W. Fuzzy-logic-based channel selection in IEEE 802.22 WRAN. *Inf. Syst.* **2015**, *48*, 327–332. [CrossRef]
35. Farahani, H.; Ebadi, M.J.; Jafari, H. Finding inverse of a fuzzy matrix using eigenvalue method. *Int. J. Innov. Technol. Explor. Eng.* **2019**, *9*, 3030–3037.
36. Jafari, H.; Malinowski, M.T.; Ebadi, M.J. Fuzzy stochastic differential equations driven by fractional Brownian motion. *Adv. Differ. Equ.* **2021**, *2021*, 16. [CrossRef]
37. Ma, L.; Wang, X.; Wang, X.; Wang, L.; Shi, Y.; Huang, M. TCDA: Truthful combinatorial double auctions for mobile edge computing in industrial Internet of Things. *IEEE Trans. Mob. Comput.* **2021**. [CrossRef]
38. Omiyi, P.E.; Nasralla, M.M.; Rehman, I.U.; Khan, N.; Martini, M.G. An intelligent fuzzy logic-based content and channel aware downlink scheduler for scalable video over OFDMA wireless systems. *Electronics* **2020**, *9*, 1071. [CrossRef]
39. Rehman, I.U.; Philip, N.Y.; Nasralla, M.M. A hybrid quality evaluation approach based on fuzzy inference system for medical video streaming over small cell technology. In Proceedings of the 2016 IEEE 18th International Conference on e-Health Networking, Applications and Services (Healthcom), Munich, Germany, 14–16 September 2016; pp. 1–6.
40. Jamali, N.; Sadegheih, A.; Lotfi, M.M.; Wood, L.C.; Ebadi, M.J. Estimating the depth of anesthesia during the induction by a novel adaptive neuro-fuzzy inference system: A case study. *Neural Process. Lett.* **2021**, *53*, 131–175. [CrossRef]
41. Balasubbareddy, M.; Sivanagaraju, S.; Suresh, C.V. Multi-objective optimization in the presence of practical constraints using non-dominated sorting hybrid cuckoo search algorithm. *Eng. Sci. Technol. Int. J.* **2015**, *18*, 603–615. [CrossRef]
42. Lee, C.C. Fuzzy logic in control systems: Fuzzy logic controller. I. *IEEE Trans. Syst. Man Cybern.* **1990**, *20*, 404–418. [CrossRef]
43. Rappaport, T.S.; MacCartney, G.R.; Samimi, M.K.; Sun, S. Wideband millimeter-wave propagation measurements and channel models for future wireless communication system design. *IEEE Trans. Commun.* **2015**, *63*, 3029–3056. [CrossRef]
44. Rahim, H.M.; Leow, C.Y.; Rahman, T.A. Millimeter wave propagation through foliage: Comparison of models. In Proceedings of the 2015 IEEE 12th Malaysia International Conference on Communications (MICC), Kuching, Malaysia, 23–25 November 2015; pp. 236–240.
45. Zhang, Y.; Anderson, C.R.; Michelusi, N.; Love, D.J.; Baker, K.R.; Krogmeier, J.V. Propagation modeling through foliage in a coniferous forest at 28 GHz. *IEEE Wirel. Commun. Lett.* **2019**, *8*, 901–904. [CrossRef]